https://doi.org/10.5194/bg-2022-100
Preprint. Discussion started: 24 May 2022

Biogeosciences Discussions

Interdisciplinary strategy to survey phytoplankton dynamics of a eutrophic lake under rain forcing: description of the instrumental set-up and first results

Fanny Noirmain[1], Jean-Luc Baray[2], Frédéric Tridon[3], Philippe Cacault[4], Hermine Billard[1], Guillaume Voyard[5], Joël Van Baelen[6], Delphine Latour[1]

Correspondence to: Fanny Noirmain (fanny.noirmain@gmail.com)

[1]Université Clermont Auvergne, CNRS, Laboratoire Microorganismes : Genome, Environnement (LMGE), UMR6023, Clermont-Ferrand, France
[2]Université Clermont Auvergne, CNRS, Laboratoire de Météorologie Physique (LaMP), UMR6016, Clermont-Ferrand, France
[3]Department of Environment, Land and Infrastructure Engineering, Politecnico di Torino, Turin, Italy
[4]Université Clermont Auvergne, CNRS, Observatoire de Physique du Globe de Clermont Ferrand (OPGC), UAR833, Clermont-Ferrand, France
[5]Université Clermont Auvergne, CNRS, Institut de Chimie de Clermont Ferrand (ICCF), UMR6296, Clermont Ferrand, France
[6]Université de la Réunion, CNRS, Météo-France, Laboratoire de l'Atmosphère et des Cyclones (LACy), UMR8105, St Denis de la Réunion, France

Abstract

We present an interdisciplinary investigation of the links between rain macro and microphysical properties, meteorological parameters, and a mountain lake to assess the impact of precipitation events on phytoplankton dynamics and, in particular, on cyanobacteria. In order to document this interdisciplinary scientific question, the Aydat lake in the French massif central mountains has been instrumented in 2020 with a set of high-resolution atmospheric radars, disdrometer, and precipitation collector. In parallel, the lake was monitored with a suite of sensors and water sampling. To illustrate the potential of this original experimental setup, we present a rain case study that occurred in September 2020 and during which three contrasted sub-periods were identified. Using our high temporal-resolution monitoring, we show that the air mass origin mainly influences the rain nutrient composition, which depends on the type of rain, convective or stratiform. Our results also highlighted a non-negligible presence of photosynthetic cells in all rains, but their very low abundance can probably not impact the phytoplankton dynamics. Nevertheless, rain events indirectly impacted phytoplankton assemblages. Indeed, among all phytoplankton genera, three cyanobacteria, *Microcystis*, *Coelomoron*, and *Merismopedia*, showed a similar pattern with a systematic punctual decrease of their abundance at the lake surface immediately after rain events, suggesting a different impact of rain events according to the cyanobacterial genus considered. These various phytoplankton responses subjected to the same rainfall event could play a key role in phytoplankton dynamics in the temperate zone. Our results highlight the interest in high-frequency and time resolution monitoring of both atmosphere and lake to better understand the cyanobacteria adaptive strategies following rain events.

https://doi.org/10.5194/bg-2022-100
Preprint. Discussion started: 24 May 2022

1. Introduction

Global warming impacts the Earth's surface temperature, which has increased globally more than1°C since the pre-industrial period. In addition to this long-term warming trend, most climatic predictions point to extreme events for many regions, including an increase in frequency and intensity of heavy precipitation for several regions located in northern Europe (Stocker and Intergovernmental Panel on Climate Change, 2013). The convective rain events are associated with low forecast probabilities due to the high spatial variability of precipitation and uncertainties in convective initiation. However, in the next decade, model simulations show that convective events could increase in frequency in South of France (Luu et al., 2020).

In parallel, water quality and preservation of biodiversity are the main concerns of the 21st century. Lakes are vulnerable to climate change and are subject to a trophic state shift towards an increased degree of heterotrophy as a result of global warming (Jennings et al., 2012). A recent lake modeling study predicts that one-third of the 365 worldwide analyzed lakes will experience a warming of the lake's surface water responsible for a change in the lake mixing regime (Woolway and Merchant, 2019). Some European lakes already present an earlier thermal stratification in the season with an increase in water stability, favoring a decrease of hypolimnetic oxygen concentrations and mixing resistance (Schmid et al., 2014; Stockwell et al., 2020; Whitehead et al., 2009; Wilhelm and Adrian, 2008).

These conditions associated with transient nutrient microenvironments in the water column benefits phytoplanktonic species, especially in favor of buoyant cyanobacteria (Jöhnk et al., 2008). Pearl and colleagues reported that increased lake water temperature, thermal stratification, and water column stability promoted cyanobacterial blooms (Paerl and Barnard, 2020). Therefore, cyanobacteria proliferation could increase due to global climate change.

Extreme events impact also the lake's abiotic factors and change the lake's physical conditions. As suggested in case studies realized on lakes located in Europe, North America, and Asia, abiotic changes can last between days to years, depending on the severity of the meteorological drivers and also on site-specific factors (Jennings et al., 2012; Knapp and Milewski, 2020; Stockwell et al., 2020). Nevertheless, contrasting results have been reported after rain events: illustrated by a temporary disruption of cyanobacterial blooms due to flushing and de-stratification, or on the contrary, an increase or recovering of cyanobacteria biomass, according to the seasonal timing, intensity, and frequency of rain events, lake geomorphology, and land use catchment (Reichwaldt and Ghadouani, 2012; Richardson et al., 2019; Rooney et al., 2018; Stockwell et al., 2020; Znachor et al., 2008).

Some studies support the theory that lake abiotic changes after rainfall events will lead to favorable conditions for cyanobacterial growth due to a more significant nutrient input after drought periods, combined with potentially more prolonged periods of high evaporation and stratification (Coumou and Rahmstorf, 2012; Reichwaldt and Ghadouani, 2012). Furthermore, heavy rainfall and strong wind could induce algal blooms when all the conditions are favorable, after days or weeks following rain events (Yang et al., 2016; Zhu et al., 2014). Nevertheless, most of these studies have been realized on reservoirs and lakes under subtropical climates (Barbiero et al., 1999; Gaedeke and Sommer, 1986; Jennings et al., 2012; Reynolds, 1980; Stockwell et al., 2020; Znachor et al., 2008). To date, few studies deal with the issue concerning the effect of rainfall on phytoplankton dynamics and

https://doi.org/10.5194/bg-2022-100
Preprint. Discussion started: 24 May 2022

cyanobacterial development under temperate climate (Wood et al., 2017). As their response to the rain event can be very fast, understanding the effect of precipitation events on phytoplankton dynamics needs to access high space-time resolution to follow the phytoplankton community changes and identify molecular and cellular responses. Although the use of sensors monitoring environmental parameters at high time resolution is increasingly common, to our knowledge, there is no study to date that uses high monitoring acquisition data to study the coupling between lake, precipitation, and atmospheric data.

The link between the characteristics of rain events (intensity, dynamics, microphysics) and phytoplankton dynamics, particularly at fine and local scales, is currently very little studied under temperate climate. Thus, a better understanding of the microphysics of local precipitation, coupled with measurements of the biochemical composition of rainwater and abiotic and biotic parameters of the lake, can provide new insights in this domain.

To address this question and gap the need for data in high temporal-resolution, we present the instrumental setup developed at Aydat, composed by cloud and rain profiling radars, a disdrometer, a precipitation collector, and lake temperature data loggers. In addition, *in situ* biochemical analysis and photosynthetic cells abundance were performed on lake and rain waters in order to complete the atmospheric and lake datasets. To illustrate the interest of this instrumental setup, we present a preliminary study of first results obtained during two weeks in September 2020. We selected three rain events during this period to illustrate the strategy of high temporal-resolution atmospheric monitoring, where lake sampling was realized before and after each. Finally, we discussed about the impact of rain events on the lake's physical conditions and phytoplankton dynamic.

This paper is then structured as follows: Section 2 describes the instrumental set-up deployed at Aydat lake. Section 3 presents the strategy of rain and lake monitoring. Section 4 provides the analysis the September 2020 case study.

2. Material and methods

2.1. Lake site and instrumental setup

Aydat lake (45.6°N; 2.9°E) is located in the French Massif Central, around 15 km south west of Clermont Ferrand, at 837 m above sea level (Fig. 1 A & B, Supplementary Fig. 1). It is a natural lake that was formed when the Veyre River was dammed by a basaltic lava flow 7500 years ago. It is a small eutrophic dimictic lake with 0.6 km² of total area, 300 km² of catchment area and 15 m maximal depth, with recurrent cyanobacterial proliferations. Aydat lake receives 75% input from the Veyre River and 25% of lateral supply through the shores and direct precipitation (Lavrieux et al., 2013).

The lake instrument setup comprises the HOBO data loggers located in the middle point of Aydat lake which record the temperature every 20 cm from the water surface to 2.8 m deep (Supplementary Table 1). In addition, during the lake campaign we also used punctually the YSI ProDSS Multiparameter Water Quality Meter instrument for *in situ* measurements of the dissolved oxygen and temperature profiles in the middle of the lake (Supplementary Table 2).

https://doi.org/10.5194/bg-2022-100
Preprint. Discussion started: 24 May 2022

2.2. Atmospheric instrumental setup

The atmospheric instrumental setup is located 420 m from Aydat lake. It comprises a cloud radar (Mira35c), a rain profiling radar (MRR), a disdrometer, and a precipitation collector. Atmospheric instruments are installed at Aydat in June 2020, and operational measurements have been available since September 2020. An overview of the location of the instruments is given in Fig. 1 C.

The Mira35c and the Micro-Rain-Radar MRR-pro were acquired from METEK Gmbh (http://metek.de/) corporation. They are used to describe vertical profiles of equivalent radar reflectivity, covering the range from 300 m to 15 km and from 30 m to 4 km, respectively. The Mira35c is a cloud radar profiler, a Ka-band Doppler polarimetric radar, with a center frequency of 35 GHz. The Micro-Rain-Radar MRR-pro is a rain profiling radar, a vertically looking K band (24.23 GHz) Doppler, Frequency Modulated Continuous Wave (FMCW). Both provide measurements of Doppler spectra from which the reflectivity and the vertical Doppler velocity are calculated. The cloud and rain radars provide an estimation of the rain rate and liquid water content deduced from the retrieved reflectivity and Doppler velocity profiles. Nevertheless, according to their respective wavelength, the Mira35c has better sensitivity and can detect tiny cloud drops, whereas the MRR is only sensitive to large raindrops. Their technical specifications are listed in Supplementary Tables 3 and 4.

The Parsivel² sensor, commercialized by the OTT Company, is an optical instrument designed to measure the raindrops' diameter and fall speed. The measurement is made when drops intersect a laser beam with a final sampling surface of 54 cm². The diameter of droplets is estimated from the decrease in the intensity of the laser beam received by a photoelectric diode, and the fall speed is estimated by the time taken by the drop to cross the beam. Rain rates are calculated by integrating the number and size of drops.

As the MRR, The Parsivel² provides the drop size distribution, i.e., the concentration of raindrops per unit volume per unit size interval (N, in m^{-3} mm^{-1}). Nevertheless, for the Parsivel², the DSD is obtained at 3 m from the ground level whereas for the MRR we obtained vertical profiles from 30 m to 4 km. More technical specifications of the Parsivel² are detailed in the supplementary Table 5.

The precipitation collector, used to collect the rain, is an automated wet-deposition sampler Eigenbrodt NSA 181/S commercialized by the Ecomesure company. It is equipped with a sensor to open the system when precipitation occurs, preventing contamination by dry deposition between precipitation events. When the sensor detects the rain, the funnel door opens and collects rainwater on a 500 cm^2 area, and water passing by the tipping bucket system counts in separate tips. The carousel holds 16 collection bottles allowing a sequential sampling of rainwater. We recorded parameters to define a rain event: first, the minimal amount of rain to start a new acquisition is 0.15 mm (i.e., three tips) to open the funnel; second, a new bottle is replaced if the maximal quantity of rain per bottle is exceeded (i.e., 250 ml/bottle) and finally, after 15 minutes without rain, we considered the rain event's end and the collector replaced the bottle by a new empty bottle. According to the recorded tips, the collected sample volume can be divided by the collection area (500 cm²) to derive the precipitation rate. In addition, the PCB reader allows us to know the hour of sampling and the duration. The technical specifications are listed in Supplementary Table 6.

https://doi.org/10.5194/bg-2022-100
Preprint. Discussion started: 24 May 2022

Biogeosciences
Discussions
Open Access
EGU

In addition, the air temperature (°C) and the wind speed ($m.s^{-1}$) are recorded by the Meteo France weather station located at Saint-Genès-Champanelle, around 7 km north east from Aydat.

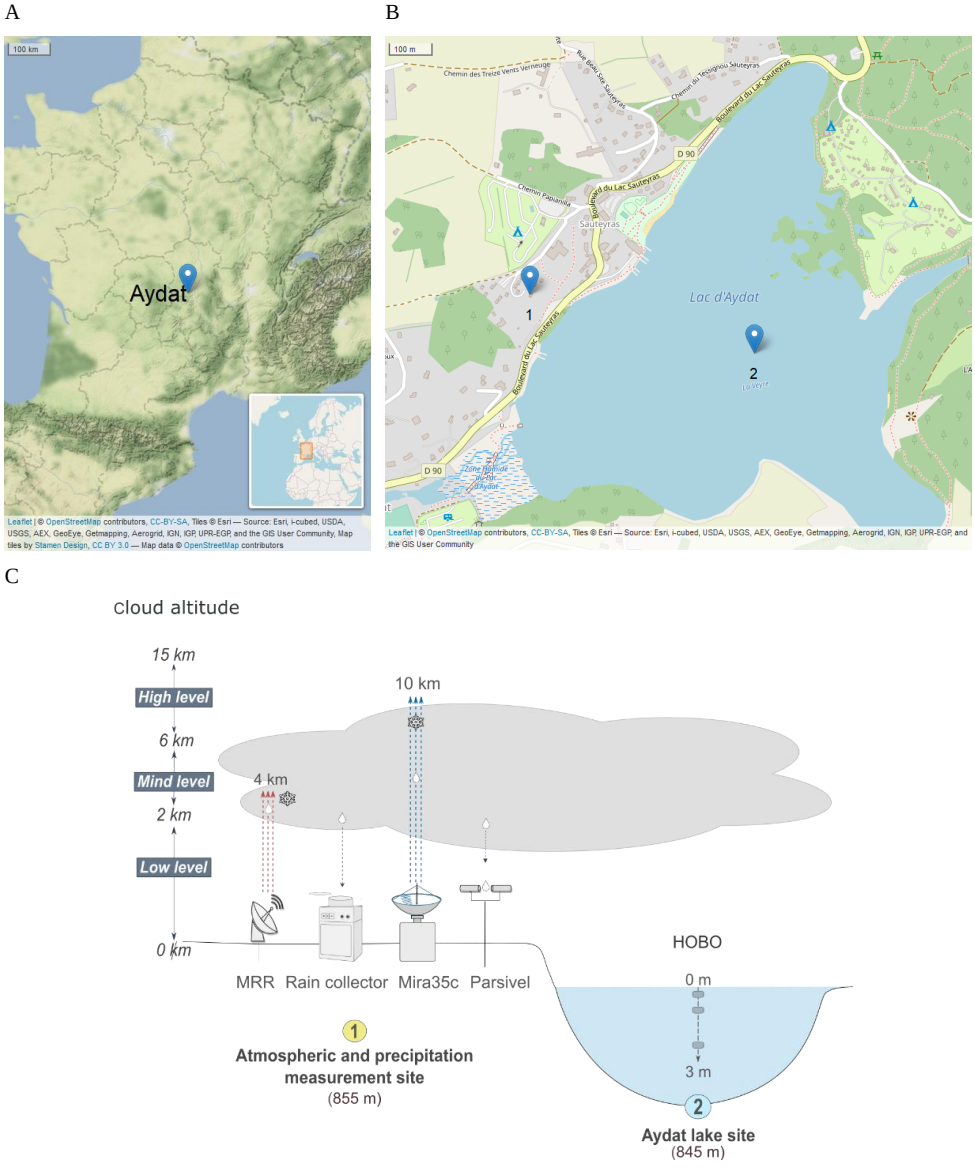

Fig. 1: (A) Cartography of Aydat town, a commune in the Puy-de-Dôme department in Auvergne-Rhône-Alpes in central France. (B) Cartography of the Aydat lake where stands the instrumental setup which comprises (1) the atmospheric and precipitation measurement site and (2) the Aydat lake site (C) Conceptual diagram of Aydat instrumental setup. OpenStreetMap data is available under the Open Database license

https://doi.org/10.5194/bg-2022-100
Preprint. Discussion started: 24 May 2022

(https://opendatacommons.org/licenses/odbl/). Maps are released under the Creative Commons Attribution-ShareAlike 2.0 (CC-BY-SA 2.0) license (https://creativecommons.org/licenses/by-sa/2.0/).

2.3. Rain and lake monitoring

The monitoring of the rain and Aydat lake started on 18th September 2020. Since then, all rains have been collected with the precipitation collector and analyzed. The infra-samples of rain waters were collected in separated bottles to perform a sequential sampling. The lake samples were collected before and after each rain period.

In this paper, to illustrate the potential of the instrumental setup, we focus on two selected rain periods of particular interest: a first from 19th until 21st September 2020, named "Rain Period 1" and a second from 24th until 28th September 2020, named "Rain Period 2" (Fig.2). Within these rain periods, we have selected three separate rain events to illustrate the strategy of high-resolution atmospheric monitoring. First, we selected one rain event occurring on 20th September 2020 from 14:00 until 16:00 UTC, named "High-Intensity-Short-Rain (HIR)" because of high rain rate observed during a short duration. Then, on the second rain period, we selected the longest event of this period, named "Continuous rain event 1 (CR1)" occurring on 27th September from 03:50 until 01:28 UTC on 28th, and "Continuous rain event 2 (CR2)", occurring 20 minutes after CR1 at 01:50. We considered the CR1 and CR2 different rain events as the drought period exceeded 15 min between them. The lake was monitored on 18th and 21st September, and on 23rd and 30th September at three depths, 0, 1.5, and 3 m in the middle of the lake (Fig. 2).

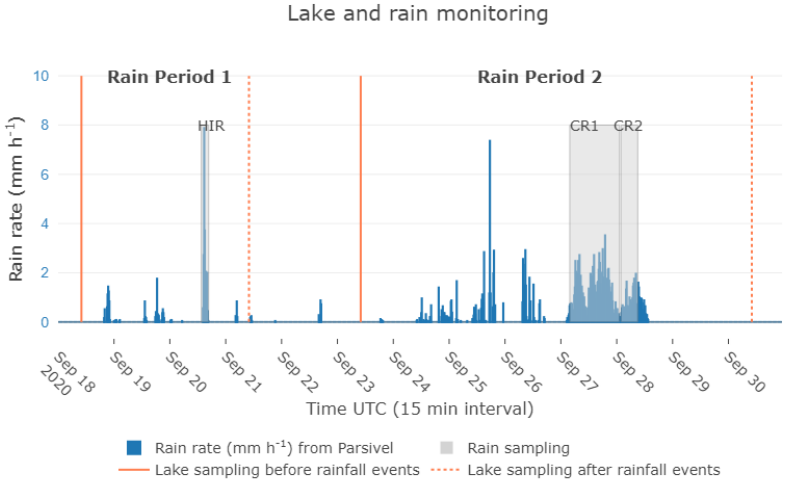

Fig. 2. Rain rate intensity from the Parsivel² sensor measured at Aydat instrumental site, within a 15 minutes interval. Lake sampling are indicated by orange line, the continuous orange lines indicate sampling performed before rainfall events, and dotted orange lines represent samplings performed after rain events. All samplings were performed in the morning between 08:00 and 10:00 UTC. Grey areas indicate the rain samplings and their duration, recorded from the Rain sensor. HIR belong to the Rain Period 1 and CR1/CR2 belong to the Rain Period 2.

https://doi.org/10.5194/bg-2022-100
Preprint. Discussion started: 24 May 2022

2.4. Sampling analysis

The rain samples were analyzed within 48 hours after the rain event stopped. We immediately measured the pH onto fresh rain samples and quantified the number of photosynthetic cells by flow cytometry. Finally, we stored 10 ml at -20°C the rainwater until we measured by ion chromatography the dissolved nutrients.

In parallel, the lake water was immediately filtered in the laboratory into sterile containers by membrane filtration with a 10-µm nylon membrane. The filtrates were stored at -20°C until we measured the dissolved nutrient in lake samples, using the same procedure for the rainwater. Then, onto fresh lake samples, the phytoplankton biomass and diversity were quantified using a Lugol's iodine solution following the counting process of the European Standard NF15204 (AFNOR, 2006). One sample per depth for each date was analyzed. The mean relative abundance of phytoplankton was normalized using the square root of cells concentration.

The dissolved nutrients, Ca^{2+}, K^{+}, Mg^{2+}, Na^{+}, NH_4^{+}, Cl^{-}, SO_4^{2-}, and NO_3^{-}, onto rain and lake waters was measured by ion chromatography using a DIONEX ICS6000 chromatograph. Ion chromatography (IC) analysis was performed employing a Dionex ICS-6000 equipped with an IonPac AG11-HC (guard-column, 2 × 50 mm) and an IonPac AS11-HC (analytical column, 2 × 250 mm) for anions and with an IonPac CG-16 (guard-column 2 × 50 mm) and an Ion-Pac CS16 (analytical column 2 × 250 mm) for cations. The elution conditions are gradient mode of KOH (1 mM to 60 mM in 35 minutes, flow rate 0.36 ml/min) for anions and isocratic mode of MSA (MethaneSulfonic acid at 30 mM, flow rate 0.25 ml/min). Chromatograms were recorded with a conductimetric cell detector with Chromeleon 7.2 software (Thermo Scientific). The nutrient concentrations were measured in triplicate.

We developed an original methodology by flow cytometry to quantify the low number of photosynthetic cells in each rain sample. After each rain event, a blank was systematically performed by passing sterile water into the rain sensor after cleaning with detergent, alcohol, and sterile water. Within two days following the rain events, rain and blank samples were 100-fold concentrated by ultra-fast-filtration (Vivaspin® 100 kDa). First, the membranes fitted to Vivaspin® concentrators were systematically pre-rinsed with 15 ml of Milli-Q water. Then the rain sample was concentrated twice by repeated centrifugations with 15 ml of rainwater in the same Vivaspin® concentrator for 25 min at room temperature (3000 x g). Finally, the concentrate was diluted in sterile Tris-EDTA (TE) buffer before counting the photosynthetic cells by flow cytometry (BD FACSCalibur™).
We used different emission sources and excitation detectors channels to distinguish specific pigment populations. Indeed, the total photosynthetic cells were quantified using an air-cooled argon-ion laser, exciting the cells at 488-nm and collecting fluorescence emission with the FL3 detector (670 Long Pass), a proxy of chlorophyll-containing cells populations, not discriminating with the other photosynthetic pigments and bioaerosols (i.e., pollen) emitting fluorescence in this range. In order to distinguish the photosynthetic pigments, the phycocyanin-rich cells were precisely quantified using a ≈635-nm red diode with an FL4 detector (661/16 Band Pass), whereas the phycoerythrin-rich cells were specially analyzed using the 488-nm laser in association with the FL2 (585/42 Band Pass) detector.
The analysis steps consisted of creating a first bi-parametric cytogram by selecting FL3 vs. SSC (side scatter) channels, to set the "total pigment" population by excluding unwanted debris. Then, from the previous "total

https://doi.org/10.5194/bg-2022-100
Preprint. Discussion started: 24 May 2022

pigment" population, we created a second cytogram using FL3 vs. FL2 channels to set the "phycoerythrin" population. Finally, the last plot was created from the inverted "phycoerythrin" gate by selecting FL3 vs. FL4 channels to set two independent and specific gates for the "chlorophyll" and "phycocyanin" populations. All gates were systematically calibrated with appropriate phytoplankton species.

The acquisition was performed in high flow rate mode for 60 seconds with detection thresholds applied on FL3 and FL4. Voltage adjustments were performed to exclude unwanted debris and appropriately place the populations of interest.

The exact flow rate was determined with Milli-Q water for each rain sample through the acquisition time and the gravimetric loss from the water sample. Data were acquired in BD CellQuest Pro software and analyzed with BD FACSDiva 9 software (Becton, Dickinson).

2.5. Statistical analysis

The Kruskal Wallis test was performed to compare if the nutrient concentrations in the rainwater differed between the rain events and between CR1 infra-samples, partitioned into three sub-periods according to the evolution reflectivity (Z) from the Mira35c. The same analysis was performed between the date of lake sampling to compare the difference of the lake nutrient concentrations before and after a rain period. The Dunn test with Bonferroni correction was applied when the Kruskal Wallis test showed a statistical difference.

The Spearman's rank correlation test evaluated correlations between environmental variables and the lake temperatures variations recorded with the HOBO sensors during the rain events.

2.6. Back trajectory measurements

We also investigate the air mass history of each rain event using the CAT model. The CAT model is a three-dimensional (3D) forward/backward kinematic trajectory code using initialization wind fields from the recent reanalysis ECMWF ERA-5, with a bilinear interpolation for horizontal wind fields and time and a log-linear interpolation for vertical wind fields. The CAT Model has been first used to establish the footprint of the atmospheric composition measurements performed at the puy de Dôme altitude observatory (Baray et al., 2020) and then to classify the cloud sampled in synergy with chemical measurements (Renard et al., 2020).

For this work, ECMWF ERA-5 wind fields were extracted every three hours with a spatial resolution of 0.5° in latitude and longitude, on 29 vertical pressure levels between 50 and 1000 hPa. Back trajectories starting at different altitudes corresponding to cloud layers observed on Mira35 radar profiles have been calculated, with a temporal resolution of 15 minutes and a total duration of 120 hours. In addition to back trajectory plots, the global origin is quantified by counting the number of trajectory points in each of the following nine geographic sectors: north-northeast (NNE), east-northeast (ENE), east-southeast (ESE), south-southeast (SSE), south-southwest (SSW), west-southwest (WSW), west-northwest (WNW) and north-northwest (NNW), and one nearby area. Points located over land and sea are also counted, by separating those which are close to the ground from those which are in the free troposphere, taking as a limit 2 km above the ground.

https://doi.org/10.5194/bg-2022-100
Preprint. Discussion started: 24 May 2022

3. Results

3.1. Macro, microphysical and biochemical characterization of cloud and rain events

The three rain events considered showed different atmospheric characteristics (Table 1). Indeed, the "High-Intensity-Short-Rain (HIR)" was a shorter event characterized by high rain intensity and low wind speed with an air mass origin coming from the Atlantic west of Spain (supplementary Fig.1). Whereas CR1, occurring during the rain period 2, was the longest rain event with a high wind speed marked by an air mass origin traveling at higher altitudes from the North sectors. CR2, which followed CR1 after 20 min without rain, was characterized by similar meteorological parameters as CR1 (i.e., rain rate and wind speed), but different air mass origins influenced it (Table 1).

These three events also presented different microphysical properties, particularly between HIR and CR1/CR2. HIR can be associated with a convective type, as the drop diameter, rain rate (peak and mean intensity) and cloud reflectivity were all larger and showed higher variability during the lifetime (standard deviation) (Table 1, Fig. 3). On the other hand, CR1 and CR2 were similar to stratiform type due to the lower variability in the drop diameter distribution, rain rate, and cloud reflectivity (Table 1, Fig. 4). In addition, we reported different cloud bright band altitudes during the three events. The bright band visible in the radar data represents the ice melting layer where the Z factor is higher due to a high reflectivity from the liquid water coating of ice crystals (Li and Moisseev, 2020). During HIR, from 14:00 UTC until 15:00 UTC, the bright band was missing, as often reported during a convective event. In contrast, during CR1, the ice crystals melt, and liquid phase rain begins to fall significantly at low height, around 500 m, whereas, for CR2, the bright band can be seen at about 2000 m, further pointing to a different air mass (Fig. 3 & 4).

The chemical composition of rain (Fig. 5.A) also discriminates these rain events even if the pH is quite similar between the rain samples, between 5.79 and 5.69 (Table 1). The concentration of some major inorganic ions, K^+, NH_4^+, NO_3^-, and SO_4^{2-} were significantly higher during HIR (p-value adjusted=0.022, p-value adjusted=0.023, 0.014, 0.009, respectively) than during CR1. In particular, the concentration of SO_4^{2-} was extremely high during HIR, three times more concentrated than during CR1, reaching almost 17 mg L^{-1}. Moreover, even if CR1 and CR2 presented similar microphysical characteristics, CR1's inorganic ions concentrations differed significantly from those obtained during CR2. Indeed Cl^-, K^+,Mg^{2+},and Na^+ concentrations were significantly higher during CR2 than CR1 (p-value adjusted=0.014, 0.0048, 0.014,0.066, respectively) whereas the concentration of Ca^{2+} and PO_4^{3-} significantly decreased during CR2 (p-value=0.0073, p-value adjusted=0.022).

Despite a global low level of photosynthetic cells in rain samples, we reported a high inter-variability between rain events (Fig. 5. B). Indeed, CR1 was characterized by the highest amount of chlorophyll (3092 cell.L^{-1}) and phycocyanin- rich cells (17 cell.L^{-1}), whereas HIR was characterized by the lower amount of chlorophyll-containing cells with 1126 cell.L^{-1} and the absence of phycocyanin. However, a high intra-variability was observed during CR1, where the phycocyanin pigment was detected in only two CR1 samples during the beginning and middle of CR1's event. Finally, the phycoerythrin pigment was absent in all rain events.

https://doi.org/10.5194/bg-2022-100
Preprint. Discussion started: 24 May 2022

3.2. Sequential analysis of CR1 infra-samples

The evolution of the reflectivity (Z) from the Mira35c allowed to partitioned the CR1 event into three sub-periods: firstly, homogenous reflectivity with a high cloud above the precipitating part of the atmosphere (9/27 03:50 to 10:30 UTC) – named CR1a, then high reflectivity streaks associated with rain bands (9/27 10:30 to 20:15 UTC) – named CR1b and finally low reflectivity associated with the event weakening (9/27 20:15 - 9/28 01:28 UTC)- named CR1c (Fig. 6.A).

The mean drop diameter and terminal drop velocity decreased during the time (Table 2). The higher rain rate occurred during CR1b when the reflectivity was higher. During this second sub-event, the drop diameter and drop velocity decreased but presented higher variabilities. At the end of the event, during CR1c, the rain rate, drop diameter, and drop terminal velocity decreased, associated with the lower Z reflectivity sub-event. During CR1, the pH in rain samples also decreased from 5.6 to 5.54. The air mass origin was principally influenced by the North sectors for the three sub-events, whereas the secondary sector came from North-Est during the first two sub-events and from the North-West for the last sub-event.

The statistical analysis performed on CR1 infra-samples repartition according to the change in the cloud reflectivity showed a significant difference in the nutrient footprint between the three CR1 sub-events (Fig. 6.B). The Dunn test analysis indicated that Cl^-, NH_4^+, PO_4^{3-}, and SO_4^{2-} were significantly higher during CR1.a, the first sub-event of CR1, compared to the second sub-event, CR1.b (p-value adjusted= 0.0005, 0.0005, 0.038 and 0.0014, respectively). Whereas, Ca^{2+}, K^+, and NO_3^- significantly increased during the last sub-event, CR1.c compared to CR1.b (p-value=0.0073, p-value adjusted=0.022).

We reported a high variability of the chlorophyll and phycocyanin-rich cell concentrations according to the cloud reflectivity periods. Indeed, the abundance of photosynthetic cells containing chlorophyll-a regularly decreased between CR1a and CR1c with a start at 4371 cell. L^{-1} to 506 cell. L^{-1} at the end of the event. The abundance of cells containing phycocyanin showed similar variations with higher concentrations during CR1a et b to finally reached 0 cell. L^{-1} at the end of the event.

https://doi.org/10.5194/bg-2022-100
Preprint. Discussion started: 24 May 2022

	Rain events	"High-Intensity-Short-Rain" (HIR)	"Continuous-Rain event 1" (CR1)	"Continuous-Rain event 2" (CR2)
Rain sensor data	Date	9/20/2020	9/27/2020	9/28/2020
	Duration (hour)	2,15	21,78	7,2
	Number of rain samples	1	6	2
in situ data	pH	5,79	5,59+-0,09	5,69±0,02
Long-range provenance (CAT model)	Primary sectors (%)	WSW (71,%)	ENE (31,7%)	NNE (44%)
		SSW 15,4%)	NNE (28,8%)	ESE (33,2%)
	Trajectory points located over land/sea below 2 km of altitude (%)	above 2 km over sea (37,6%)	below 2 km over land (40%)	below 2 km over land (48%)
		above 2 km over land (27%)	Below 2 km over sea (24,3%)	below 2 km over sea (29,3%)
MRR data	Terminal Drop Velocity ($m.s^{-1}$)	5,47±2,05	4,14±1,67	4,20±1,34
Parsivel data	Mean Drop diameter (mm)	0,57	0,35	0,36
	Peak intensity (5 min interval) ($mm.\ h^{-1}$)	13.32±2.2	5.1±2.9	2.1±0.4
	Mean rain rate ($mm.\ h^{-1}$)	2.5±3.15	1.26±0.9	0.8±0.5
Meteorological data from St-Genes	Mean Air Temp (°C)	16,63±1,42	4,8±0,9	6,45±0,36
	Mean Wind speed (m/s)	1,36±0,46	4,67±0,82	3,3±0,96
HOBO	Mean Lake temperature [0-2,8 m] (°C)	19,46±0,06	14,58±0,3	13,97±0,06
	Mean water irradiance [0-2,8 m] (Lux)	328,2±158	344,2±566,7	102,4±184

Table.1: Mean characteristics of the "High-Intensity-Short-Rain" event (HIR) on 20th September from 14:00 until 16:15 UTC, the "Continuous-Rain event 1" (CR1) on 27th September at 03:50 until 28th September at 01:28, and finally the "Continuous-Rain event 2" (CR2) on 28th September at 01:50 until 09:00 UTC. Macro and microphysical data were recorded at the Aydat instrumental site using the Rain sensor, Parsivel, and MRR instruments. Meteorological data come from Saint-Genes Champanelle Météo-France weather station. Mean lake water temperature and light intensity during rain events were recorded from the HOBO data loggers.

https://doi.org/10.5194/bg-2022-100
Preprint. Discussion started: 24 May 2022

	CR1's sub-events	CR1.a	CR1.b	CR1.c
Rain sensor data	Date time (UTC)	9/27/2020 03:50	9/27/2020 10:30	9/27/2020 20:35
	Number of CR1's infra-samples	2	3	1
	Duration (hour)	6,4	10,05	4,5
in situ data	pH	5,59±0,1	5,63±0,1	5,54
Long-range provenance (CAT model)	Primary sectors (%)	NNE (32.5 %)	ENE (33.7%)	ENE (32.5%)
		ENE (29.7%)	NNE (30.8%)	NWW(25.5%)
	Above or below 2 km over land or sea (%)	below 2 km over land (34%)	below 2 km over land (50%)	below 2 km over land (39%)
		Above 2 km over sea (26.2%)	Below 2 km over sea (28.3%)	Below 2 km over sea (28.3%)
MRR data	Terminal Drop Velocity (m s^{-1})	5±0,96	4,5±1,6	2,16±0,7
Parsivel data	Rain amount (mm)	8.74	15.28	3.27
	Peak intensity (5 min interval) (mm. h^{-1})	3.3±0.21	5.1±2.97	2±0.17
	Mean drop diameter (mm)	0.47	0.36	0.29
Meteorologial data from St-Genes	Mean Air Temp (°C)	5,31±-1,13	6,44±1,32	5,9±0,2
	Mean Wind speed (m s^{-1})	4,15±1,2	4,04±1,31	4,26±0,4
Lake data from HOBO	Mean water temperature [0-2.8 m] (°C)	14.92±0.1	14.55±0.18	14,16±0.05
	Mean water light irradiance [0-2.8 m] (Lux)	408.85±551	470±648	0.0±0.02

Table 2: Mean characteristics of CR1's infra-samples collected on 27th September at 03:50 UTC until 28th September at 01:28 UTC. Sub-divisions were according to the evolution of the reflectivity (Z) from Mira.

https://doi.org/10.5194/bg-2022-100
Preprint. Discussion started: 24 May 2022

A

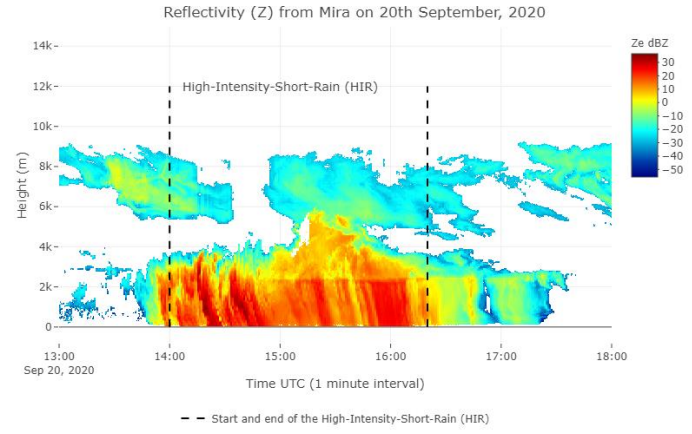

B

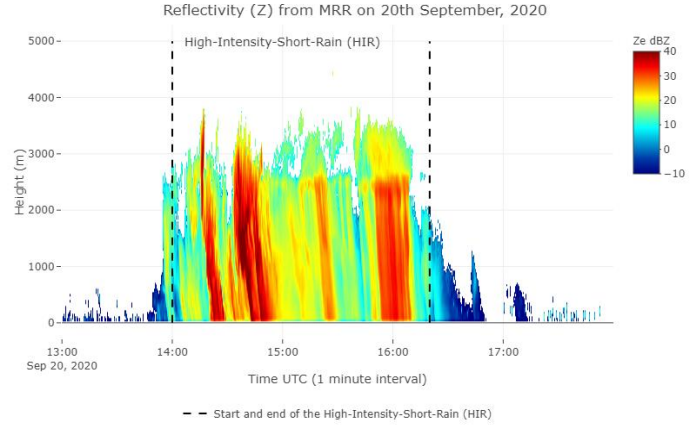

Fig. 3*:* Time series of vertical profiles of radar equivalent reflectivity on 20th September from 13:00 to 18:00 UTC, (A) with Mira35c, with a temporal resolution of 5 seconds, (B) with MRR.

https://doi.org/10.5194/bg-2022-100
Preprint. Discussion started: 24 May 2022

A

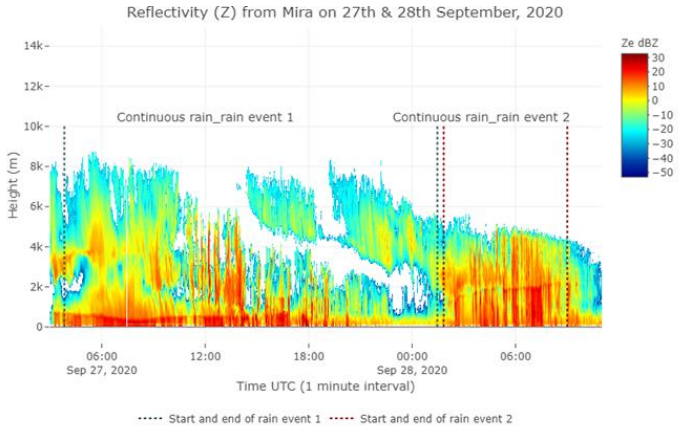

B

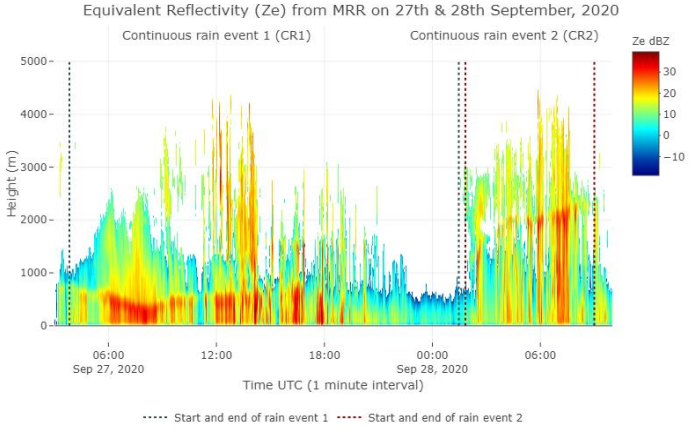

Fig. 4: Time series of vertical profiles of the radar equivalent reflectivity from 27th September 03:50 to 28th at 9:00 UTC, (A) with Mira35c, with a time resolution of 5 seconds. (B) with the MRR sensor within an interval of 5 seconds.

360

https://doi.org/10.5194/bg-2022-100
Preprint. Discussion started: 24 May 2022

A

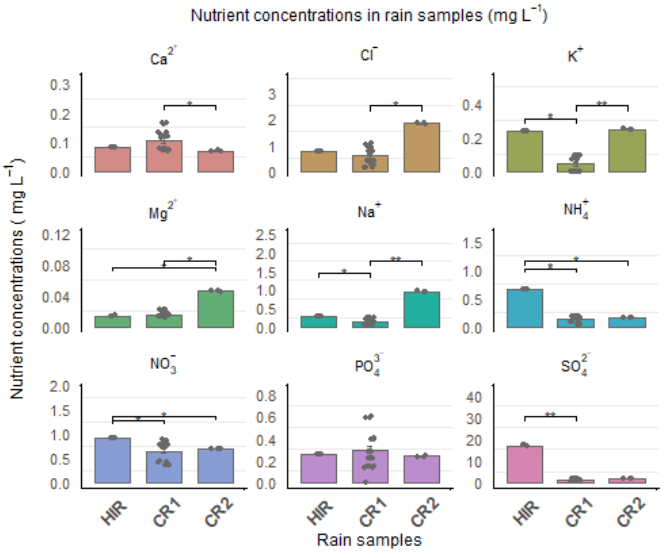

B

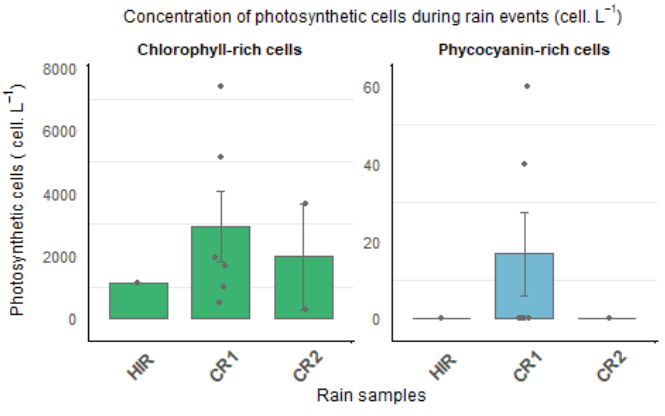

Fig. 5: (A) Inorganic anions and cations concentrations (mg. L^{-1}) and (B) Photosynthetic cell concentrations (cell. L^{-1}) during HIR, CR1 and CR2. The significance level was reported from the Dunn test to compare the nutrient concentration between rain events.

365

https://doi.org/10.5194/bg-2022-100
Preprint. Discussion started: 24 May 2022

A

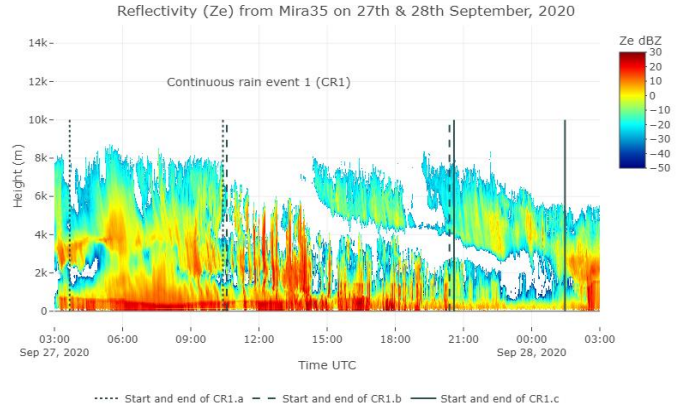

B

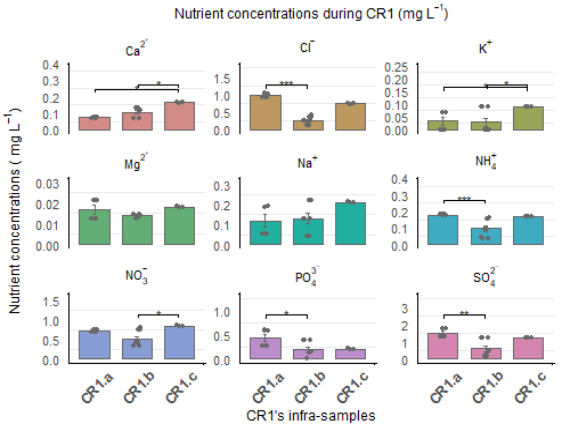

C

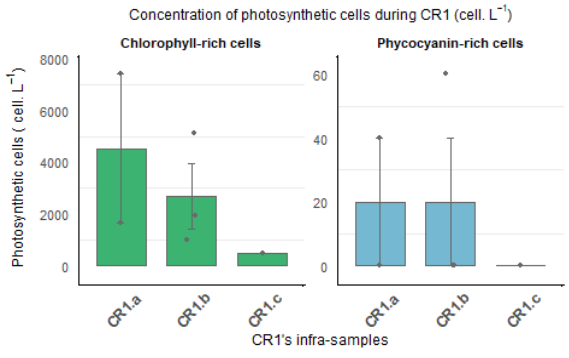

Fig. 6: (A) CR1 event partitioned into three sub-periods according to the evolution of the reflectivity (Z) from the Mira35c. (B) Inorganic nutrient concentrations (mg. L^{-1}) and. (C) Photosynthetic cell concentrations (cell. L^{-1}) during CR1's sub-events. The significance level was reported from the Dunn test to compare the nutrient concentration between CR1's sub-events.

https://doi.org/10.5194/bg-2022-100
Preprint. Discussion started: 24 May 2022

3.3. Precipitation and meteorological impacts on lake physical structuration and phytoplankton dynamic

The punctual vertical lake profile of temperature performed before and after rain periods showed differences according to the rain events. Indeed, after the first rain period, the temperature of the epilimnion (i.e., the upper layer of water in a thermally stratified lake) decreased slightly (1°C). On the contrary, after the second rain period, the epilimnion temperature decreased drastically (6°C), and the thermocline sank to 2 m below, suggesting a decrease in the vertical stability of the upper water column (thermocline strength) (Fig. 7. A).

The use in parallel of HOBO data allowed a more detailed description of the impact of rain on lake temperature structuration. For the three rain events, the mean lake temperatures were positively correlated to the mean air temperature ($r = 0.4$, p-value = $2{,}6.10^{-04}$) and negatively to the wind speed ($r = -0.53$, p-value = $1{,}36.10^{-06}$). Nevertheless, we reported a stronger significant negative correlation between the mean rain rate and the water temperature at the surface during HIR ($r = -0.7$, p-value = $1{,}246.10^{-06}$) than during CR1 ($r = -0.2$, p-value = $1.32.10^{-03}$) and CR2 ($r = -0.46$, p-value = $1{,}76.10^{-06}$). Indeed, when HIR started, the vertical temperature gradient immediately decreased - the lake surface temperature, previously warmer by 0.7°C than 2.8m deep, was reduced to only 0.26°C higher. The convective HIR was also associated with an air temperature decreasing by one degree Celsius, and with a drastic reduction of the level of water irradiance, from 4032 Lux to 555 Lux at the lake surface (Fig. 7. B). On the other hand, CR1 and CR2 started at the night's end when water surface temperature was not yet stratified. Nevertheless, as the level of water irradiance increased until 3400 Lux during CR1b, the lake temperature increased at the surface, to become warmer by 0.4°C than 2.8 m deep. In contrast, all depths presented similar temperatures during CR2 associated with a low water irradiance level (526 Lux) (Fig. 7. C & D). Interestingly, during HIR, the rain rate did not correlate significantly to the water temperature deeper than 1.6 m. In contrast, it was still correlated during CR1 and CR2 until 2.8 m deep.

In parallel to the temporary changes in the vertical thermal structure of the lake, the total phytoplankton cellular concentration decreased systematically at the lake surface, by 26 and 12% after the two rain periods, on 21st and 30th September, respectively. However, the phytoplankton decrease was less pronounced at 3 m deep after the rain period 1, whereas it was less pronounced at 1.5 m deep after the rain period 2 (Fig. 8.A). Between the two rain periods, the phytoplankton abundance increased by a factor of two at the surface and 1.5 m deep, and by 37% at 3 m deep. The abundance of bacillariophytes, charophytes, cryptophytes, and chlorophytes showed moderate variations during the lake campaign and between the rain events. In contrast, the cyanobacteria concentrations showed high temporal variability (Fig. 8.B). Nevertheless, among all the cyanobacteria genus, only three of them were significantly affected by the rain: *Microcystis*, *Coelomoron*, and *Merispomedia*, which decreased systematically after the two rain periods. For example, *Microcystis* abundance decreased between 60 and 72 % at all depths after HIR, and between 57 and 81 % at all depths after CR.

Finally, the nutrient concentrations varied differently after the rain events. Among the anions, the SO_4^{2-} concentration systematically increased after the two rain periods, mainly after rain periods 2, by 24 and 32 % at the surface and 1.5 m respectively. On the contrary, NO_3^- significantly decreased after the two rain periods, by 90% at 1.5 m after RP1 (Fig. 8.C). Among the cations, Ca^{2+}concentration systematically increased after the two rain periods, between 6 to 19% depending on the depths (Fig. 8.D), whereas NH_4^+ significantly increased at

https://doi.org/10.5194/bg-2022-100
Preprint. Discussion started: 24 May 2022

the surface after RP1, and at all depths after RP2. On the other hand, Mg^{2+},Cl^{-}, K^{+}, Na^{+}, and PO_4^{3-} concentrations presented important variations among the depths and the rain periods.

A

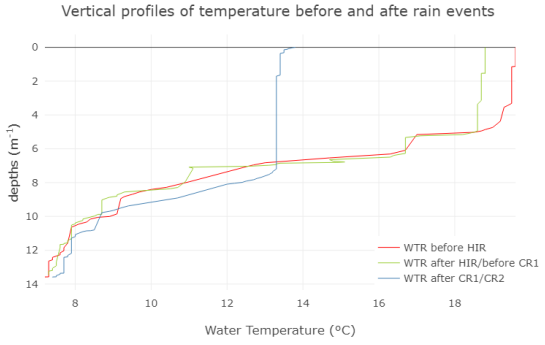

B

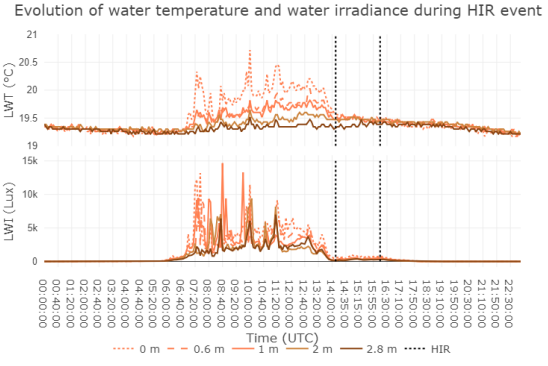

C

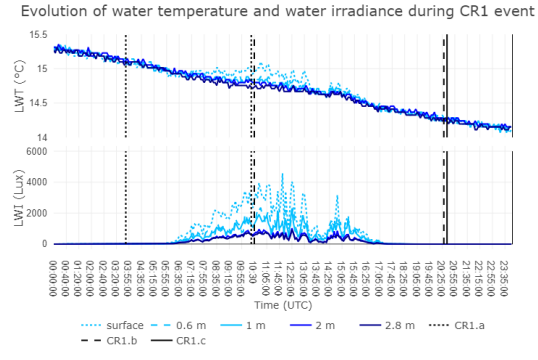

https://doi.org/10.5194/bg-2022-100
Preprint. Discussion started: 24 May 2022

D

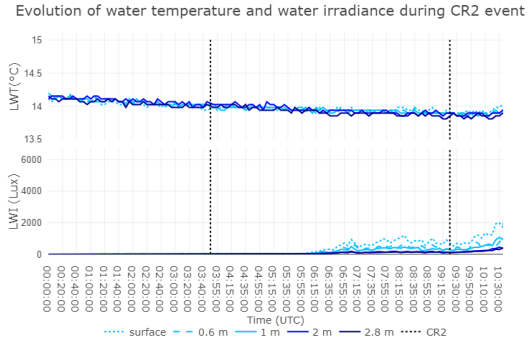

Fig. 7: (A) Water temperature vertical profiles into the lake water column before and after rain events, recorded with the YSI ProDSS probe on 18th (red line), 23th (green line), and 30th (blue line) September 2020. The continuous lines correspond to the oxygen profiles (ODO) in mg L^{-1} and dotted lines correspond to the water temperature (WT) in Celsius degrees. (B) Lake water temperature (LWT) and lake water irradiance (LWI) at the surface and down to 2.8 m of depth recorded with the HOBO (5 min resolution) before, during, and after HIR, (C) and CR1 (D) CR2.

A

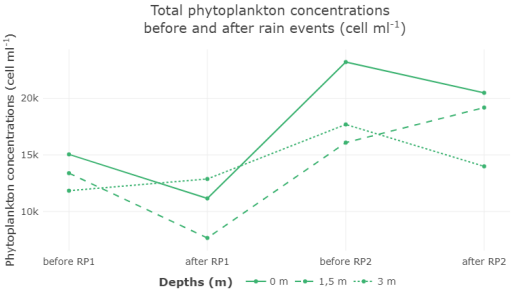

https://doi.org/10.5194/bg-2022-100
Preprint. Discussion started: 24 May 2022

B

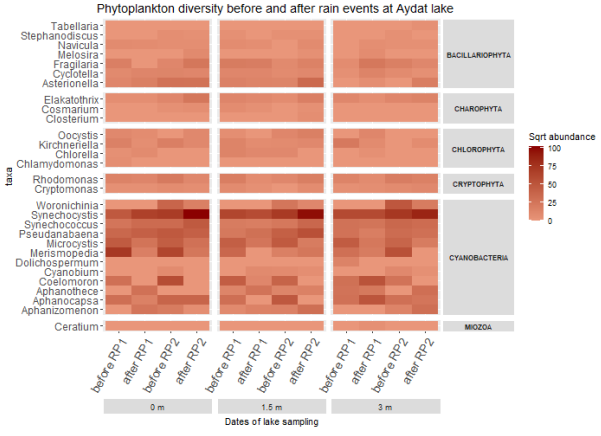

C

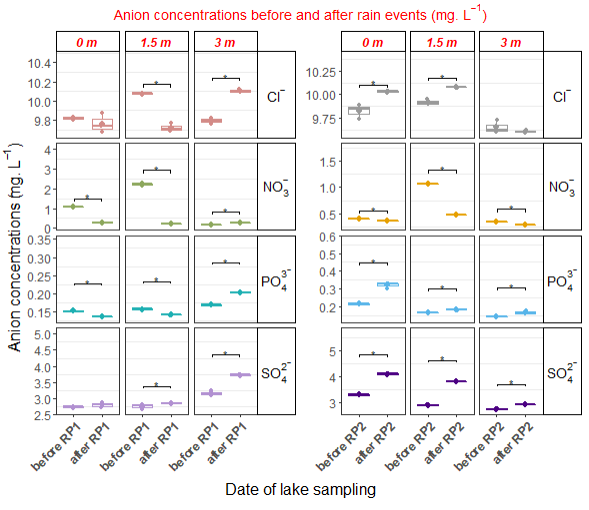

https://doi.org/10.5194/bg-2022-100
Preprint. Discussion started: 24 May 2022

D

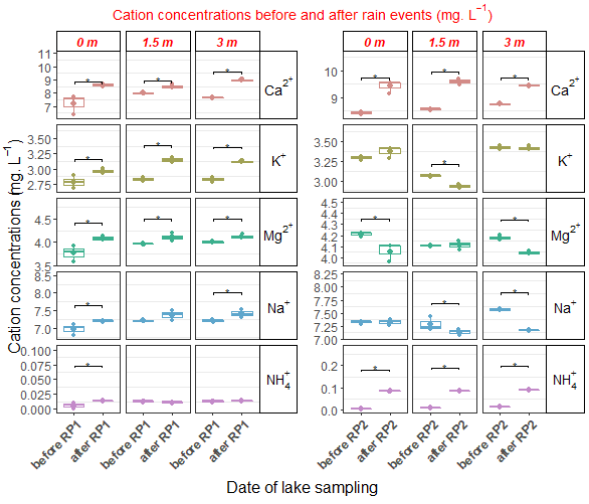

Fig. 8: Temporal evolution of (A) the total phytoplankton cell concentration (cell. ml^{-1}) (B) the mean relative Phytoplankton abundance (square root transformed) (C) the mean anion concentrations (mg. L^{-1}) and (D) the mean cation concentration into lake samples collected at three depths into Aydat lake before and after Rain Period 1 (RP1), where HIR event occurred, and before and after Rain Period 2 (RP2), where both CR1 and CR2 events occurred.

4. Discussion

4.1. Variation in the biochemical composition of rain samples according to the meteorological, macro, and microphysical properties of rain

Our instrumental site allows the real-time characterization of rain events and provides a new data set to understand the atmospheric processes influencing the biochemical rain compositions. Using the high temporal-resolution monitoring, we report that the biochemical rain compositions were influenced by different atmospheric processes depending on the type of rain, convective or stratiform. The chemical rain composition depends on the long-range transport of chemical species by clouds and on local scavenging of atmospheric aerosols during the rain event (Bertrand et al., 2008). Our preliminary results seem to indicate that long-range transport could be one of the main factors influencing the chemical composition of stratiform rain, while local scavenging could be predominant during convective rain. Indeed, most anthropogenic ions were reported during HIR with 99% of SO_4^{2-} from an anthropic origin (based on the SO_4^{2-} ratio to Na^+) (Itahashi et al., 2018). This concentration is very high compared to those obtained in polluted and continental clouds reported in a long-term study performed at the Puy de Dôme station in France (PUY) (Deguillaume et al., 2014) located 16km from Aydat. Furthermore, due to the higher HIR's drop diameter, convective rain could wash out nutrients from the air column more efficiently than during a stratiform event. These results suggest that SO_4^{2-} concentration could be provided from a local source at the proximity of Aydat.

https://doi.org/10.5194/bg-2022-100
Preprint. Discussion started: 24 May 2022

On the other hand, the chemical composition of the stratiform CR event seems highly impacted by the air mass origin. Indeed, closer in time, CR1 and CR2 events have similar microphysical properties (i.e., mean drop diameter and cloud reflectivity) and occurred during similar meteorological conditions. Nonetheless, they have different biochemical footprints associated with a long-range transport coming from different backward trajectories. Indeed, CR1 was marked by anthropogenic sources, agreeing with east-northeast and north-northeast air mass origins reported as "polluted" and "continental" cloud categories, whereas CR2 was mainly influenced by marine ion composition in agreement with the east-southeast air mass origin, reported as the "marine" cloud category (Deguillaume et al., 2014; Renard et al., 2020). We can hypothesize that for stratiform events, the long-range transport could mainly impact the chemical composition of rain, in parallel to meteorological variables and physical properties of clouds and rains.

The sequential analysis performed with high-time resolution on CR1's infra-samples confirmed this hypothesis. Indeed, whereas meteorological conditions stayed stable, we reported a nutrient reloading at the end of CR1 instead of an expected continual decrease in the nutrients concentration in rain samples. This nutrients reloading, charged in K^+ and Ca^{2+}, was associated with the new secondary air mass coming from the North-West sectors. However, the rain did not fall directly from the new air mass but from the cloud below, suggesting that one part of the nutrient composition came from the ascendant fluxes by dry deposition. This result suggests that dry depositions should also be considered in addition to the wet deposition to better estimate the fluxes in the atmosphere.

Long-range transport or local scavenging of the atmosphere could also impact the rain photosynthetic cells concentration. However, information about the microalgae and cyanobacteria in the rainwater is scarce in the literature, and the scavenging process is little understood (Dillon et al., 2020; Wiśniewska et al., 2022). Moreover, only two publications reported microalgae and cyanobacteria in the rainwater and the results as well the methodology used were different. Flow cytometry was used in both studies to estimate the concentration of cells containing chlorophyll—nevertheless, the authors used rainwater after 30 days of culturing (Wiśniewska et al., 2022) or fresh samples (Dillon et al., 2020) to perform the analysis. The culture of aerial or rainfall species should be avoided as previous studies reported troubles with aerial bacteria's cultivability depending on the majority of the strain and growth medium used (Burrows et al., 2009). In addition, by flow cytometry, Dillon and colleagues used the FL3 channels to detect the concentration of chlorophyll-containing cells, but other bioaerosols, especially the pollen, present a strong auto-fluorescence in the same wavelength emission range as photosynthetic cells. Therefore, as the pollen during springtime thunderstorms can be very high and washed out from the air column by the rain (Hughes et al., 2020), it can artificially increase the chlorophyll amount in the rainwater (Negron et al., 2020). So, in this context, with only a few studies on this topic and the lack of appropriate methods to detect the rain concentration of microalgae and cyanobacteria, more investigations are necessary to determine the number of microalgae and cyanobacteria in the rainwater and understand the key factors responsible of their washed out from the atmosphere.

By developing an innovative method using flow cytometry to separate the concentration of chlorophyll, phycocyanin, and phycoerythrin-rich cells on fresh rain samples, we bring new information about the scavenging process of photosynthetic cells in the rainwater.

https://doi.org/10.5194/bg-2022-100
Preprint. Discussion started: 24 May 2022

Our results suggest that multiple environmental factors influence the photosynthetic cell concentration in the rainwater. Indeed, we reported the higher photosynthetic cells concentration during CR1, characterized by higher wind speed, lower air mass altitude, and lower cloud's bright band elevation. In contrast, the lower photosynthetic cell concentration occurring during HIR characterized by lower wind speed, higher air mass altitude, and higher cloud's bright band elevation. Therefore, these results reinforce the supposition that the wind speed is a potential driver of aerial microalgae emitted from water reservoirs or other surfaces to the atmosphere through splash and tap mechanisms (K. Sharma et al., 2006; Rosas et al., 1989; Schlichting, 1964; Tormo et al., 2001) and also suggest that both, the cloud's bright band elevation and the air mass altitude could influence the rain microalgae concentration. Indeed, a similar analysis has already been reported suggesting that lower air mass altitude within the planetary boundary layer could be a greater source of biological aerosols due to long-range movement of air masses (Šantl-Temkiv et al., 2022).

We also reported the influence of the air mass origin on the rain photosynthetic cell concentrations, with a higher concentration of photosynthetic cells when the air mass was traveling from the Baltic Sea and a lower concentration when the air mass was traveling from Atlantic West Spain. The Baltic sea was already mentioned as a potential source of microalgae and cyanobacteria in a recent study (Wiśniewska et al., 2022). Nevertheless, Dillon and colleagues reported contrasting results, with a positive correlation between the number of chlorophyll-containing cells and the air mass originating from the West (Dillon et al., 2020).

Finally, we reported a potential link between the abundance of photosynthetic cells and microphysical rain properties during the CR1's sequential analysis. Indeed, the photosynthetic cells concentration decreased, following drop diameter and terminal velocity. Furthermore, we did not see reloading of photosynthetic cells when the new air mass was coming, suggesting that the local atmosphere could be of major influence to most cells concentrations instead of relying on cloud contribution. Nevertheless, due to the high variability and low level of photosynthetic cells abundance in our samples, this hypothesis needs to be confirmed by long-term studies to collect data set with high-resolution.

4.2. Rain impacts on abiotic and biotic variables in Aydat lake: the contribution of high-frequency data

We reported different lake temperature variations during HIR and CR events using high-frequency monitoring. Indeed, HIR affected the vertical thermal gradient by immediately reducing the thermic difference of the three first meters, and after only one hour of rain, the diurnal stratification disappeared. On the contrary, during CR1, starting at the end of the night during an unstratified period, we noticed a slight increase of the surface lake temperature by 0.4°C compared to 2.8 m deep, associated with an increase in solar radiation. Even if the difference in temperature gradient at the lake surface depends on the solar and water irradiances, the rain's physical properties can also act in the process. Indeed, the higher mean drop diameter of HIR had probably a more substantial impact on the vertical gradient of temperature than during CR1 and CR2 events, characterized by a mean drop diameter about twice as small. Indeed, the correlation strength between the mean rain rate and the lake temperature was higher during HIR than during CR1 and CR2, suggesting a stronger impact when the rain is convective. Nevertheless, according to the stability of the lake thermal stratification, this impact will be different depending of the thermocline strength. Indeed, during CR1 and CR2, the lake temperature was significantly correlated to the rain rate until 2.8 m, instead of 1.6 m deep during HIR, probably due to decreased thermal stratification strength.

https://doi.org/10.5194/bg-2022-100
Preprint. Discussion started: 24 May 2022

Previous studies reported a turbulent mixing over 10–20 cm depths with heavy artificial rainfall with a drop size of approximately 3 mm (Lange et al., 2000). Nevertheless, during rain events, the impact of the drops is not the only possible cause of effects as, numerous meteorological variables, such as air temperature, wind speed and directions, can also impact the surface mixing (Woolway and Merchant, 2019). The mechanical mixing due to heavy rain might be comparable to a strong wind, inducing a convective mixing depending on the thermal stratification (Rooney et al., 2018). However, the impact of rain on lake mixing is still little understood and its effect appears to be site-specific. Indeed, previous studies report that it could depend on the ratio between lake volume and the volume of runoff from the flood (de Eyto et al., 2016). Hence, only high-frequency monitoring with the detection variations at fine temporal and spatial scales will distinguish the impact of different types of rain on lake thermal stability.

We also compared the biochemical rain composition with that of the lake before and after the rain events to investigate if a wet atmospheric deposition could impact the lake's chemical composition. Although some nutrients in the rain were more concentrated than in the lake, we found that the wet atmospheric deposition did not directly affect the lake biochemical composition during our short study case. Indeed, after the rain period one, the concentrations of Ca^{2+}, Na^{+}, K^{+}, and Mg^{2+} increased at all depths in the lake, whereas they were between 14 and 190-fold less concentrated in rain water than in the lake surface. On the other hand, the rain and lake concentrations of NO_3^- were quite similar, whereas its concentrations decreased in the lake after the two rain periods. Therefore, these contrasted results suggest that the wet atmospheric deposition did not influence the nutrients variability in the lake and contradict previous hypothesis suggesting that wet atmospheric could increase the nutrients load in the lake. Indeed, the atmospheric deposition could enhance the dissolved organic carbon after storms (Jennings et al., 2012). To our knowledge, no study has compared the nutrients concentration in the rain with those obtained in the lake following rain events. Hence, we aim to gap the knowledge by acquiring a prolonged data set with high-frequency and high-time resolution coupled to hydrologic regimes analysis.

In addition, as all rains analyses showed the presence of photosynthetic cells in the rainwater, we wonder about the role of these micro-algae on phytoplankton dynamics. Indeed, Dillon and colleagues extrapolated a chlorophyll-containing cells flux of 10^9 and 10^{12} cells that enter the Aydat lake per rainy day, based on the photosynthetic cells count in the rainwater and the lake area estimation. They suggested that these new organisms could impact the local water quality and ecology (Dillon et al., 2020). However, this assumption did not consider the ratio between the phytoplankton biomass contained in a lake and the photosynthetic cells abundance contained in the rain. Indeed, in general, phytoplankton abundance in freshwater ecosystems ranges between 10^3 and 10^5 cells.ml^{-1} as in our study, whereas in the rainwater, the chlorophyll-containing cells are very lower and reached a maximum of 3 cell mL^{-1} in our case. So, even if considering the lake surface area, these concentrations will still be negligible compared to the total phytoplankton concentration in the lake volume. Thus, photosynthetic cells in the rain probably do not impact the phytoplankton biomass. Nevertheless, as a source of new genotypes, if these cells survive to atmospheric conditions, they could enhance the diversity of the phytoplankton of the lake even if the species currently reported in the rainwater did not correspond to those usually observed in the lake (Curren and Leong, 2020; Dillon et al., 2020; Wiśniewska et al., 2019).

https://doi.org/10.5194/bg-2022-100
Preprint. Discussion started: 24 May 2022

On the other hand, our results showed a mechanical impact of the rain on the phytoplankton dynamics. Indeed, we reported a systematic decreased of the phytoplankton concentration after rain events, linked with changes of phytoplankton assemblage. Whereas other groups stayed stable, such as charophytes and chlorophytes, interestingly, we reported a systematically decreased of the cyanobacteria *Microcystis*, *Coelomoron*, and *Merismopedia* after each rain period. These genera belong to the Lm and Lo codons (Padisák et al., 2009; Reynolds, 2006) and were reported as sensitive to mixing and flushing (Elliott, 2010; Verspagen et al., 2006). So, our results suggest that they were pulled down in deeper water during rain events, and punctually stayed in deeper layers, as confirmed by their increased concentrations at 3 m depth after RP1. Then, their recoveries were relatively quick, as in only two days after the rain period, the abundance of these three genus were similar to those of the period before raining, at all depths. It is well known that these cyanobacteria have adaptive strategies for vertical migration to the surface, in search of nutrients and light (Padisák et al., 2009; Reynolds et al., 2002; Rinke et al., 2010) due to their large surface/volume ratio and gas vesicles. Therefore, this adaptive strategy could help them to shortly recover at lake surface by adjusting their position into the water column (Wood et al., 2017).
This trend is not common to all cyanobacteria and as example, the abundance of *Synechocystis* gradually increased during the lake campaign and seems persistent with rain events. Indeed, *Synechocystis*, is a small cyanobacteria (named picocyanobacteria), with a tendency not to sink out rapidly (Reynolds et al., 2002). Moreover, Callieri noted a high growth potential of this cyanobacteria (Callieri, 2010) which is confirmed by our results with an increase of its biomass by two fold after each rain event, showing a low sensitivity to rain events. So, interestingly, our monitoring highlighted a short-term impact of the rain on phytoplankton but that can have a more lasting impact on this community and thus help to better understand their seasonal dynamics.

5. Conclusion

The interdisciplinary Aydat instrumental site allows atmospheric and lake monitoring with a high temporal resolution to improve the understanding of lake biochemical and phytoplankton dynamics following rain events with different magnitudes. In addition, it allows studying the specific impacts of rain events on the phytoplankton and cyanobacteria dynamic, which are currently poorly understood. Although many lakes are systematically monitored, the high frequency observations of both the atmosphere and lake is missing, and most studies have focused on the extreme events (de Eyto et al., 2016; Jennings et al., 2012). Our results show that these direct interactions between rain and lake are of particular interest. Indeed, during this short study case, we characterized convective and stratiform rain events, and reported their effects on abiotic and biotic lake variables. We reported that the air mass origin mainly influences the rain nutrients composition, that could depend on the type of rain. The analysis of the rapid evolution of the rain composition is only possible thanks to the high-resolution monitoring. Future studies will aim to better understand the washed-out process of nutrients and photosynthetic cells from the air column by monitoring a higher number of samples coupled to high-frequency and time resolution.

Even if our results highlighted the non-negligible presence of photosynthetic cells in all rain, their very low abundance can probably not impact the phytoplankton dynamics. However, in the case of surviving photosynthetic cells in rain events, they could enhance the diversity of the phytoplankton. Likewise, the wet atmospheric

https://doi.org/10.5194/bg-2022-100
Preprint. Discussion started: 24 May 2022

deposition did not impact the lake's inorganic nutrient variations. Furthermore, we reported that rain impacts the vertical thermal structure of the lake. The magnitude of this impact depends primarily on meteorological variables, such as solar and water radiations and air temperature, and the physical characteristics of rain events, such as the drop diameter, depending on the type of rain. Despite this different impact on thermal structuration, interestingly, three species of cyanobacteria showed similar answers after rain events: their abundance systematically decreased after rain and recovered shortly few days after, whereas other species did not similarly vary following rain events. These first findings need to be confirmed in a prolonged study to better understand the adaptabilities process of cyanobacteria. Indeed, our case study provides an example of an interesting cyanobacteria response following rain events, suggesting a different impact of rain according to the genus considered. These various responses of phytoplankton subjected to the same rainfall event are still poorly understood and must be taken into account to explain the entire dynamics of phytoplankton.

Author contributions

Fanny Noirmain: Writing - Original Draft, Conceptualization, Investigation, Visualization
Jean-Luc Baray, Joel Van Baelen & Delphine Latour: Supervision, Review & Editing, Conceptualization
Frédéric Tridon: Software-expertise
Philippe Cacault: Radar operation and data processing
Hermine Billard: Technical support-expertise
Guillaume Voyard: Resources-technical support

Conflict of interest

The authors declare there is no conflict of interest.

Acknowledgments

We thank the FRE (Fédération des Recherches en Environnement), CPER, FEDER, and CAP 20-25, which funded the atmospheric instruments. We thank "ATHOS environnement" for realizing the enumeration of phytoplankton in the lake samples and the members of Team IRTA for their help to perform lake sampling. This work was made possible with thanks to the OPGC technical staff (Frédéric Peyrin and Claude Hervier) who managed the atmospheric instruments installation. We want to thank the Plateforme CYSTEM – UCA PARTNER (Clermont-Ferrand, FRANCE) for its technical support and expertise and Mathilde Meynier for the optimization of the ion chromatography methodology. Finally, we thank «Volcans vacances" lodging, allowing a place to install the atmospheric instruments at the proximity of the Aydat lake.

References

AFNOR: NF EN 15204, in: Qualité de l'eau. Norme guide pour le dénombrement du phytoplancton par microscopie inversée (méthode Utermöhl), 39, 2006.

Baray, J.-L., Deguillaume, L., Colomb, A., Sellegri, K., Freney, E., Rose, C., Van Baelen, J., Pichon, J.-M., Picard, D., Fréville, P., Bouvier, L., Ribeiro, M., Amato, P., Banson, S., Bianco, A., Borbon, A., Bourcier, L., Bras, Y., Brigante, M., Cacault, P., Chauvigné, A., Charbouillot, T., Chaumerliac, N., Delort, A.-M., Delmotte, M., Dupuy, R., Farah, A., Febvre, G., Flossmann, A., Gourbeyre, C., Hervier, C., Hervo, M., Huret, N., Joly, M., Kazan, V., Lopez, M., Mailhot, G., Marinoni, A., Masson, O., Montoux, N., Parazols, M., Peyrin, F., Pointin, Y., Ramonet,

M., Rocco, M., Sancelme, M., Sauvage, S., Schmidt, M., Tison, E., Vaïtilingom, M., Villani, P., Wang, M., Yver-Kwok, C., and Laj, P.: Cézeaux-Aulnat-Opme-Puy De Dôme: a multi-site for the long-term survey of the tropospheric composition and climate change, Atmospheric Meas. Tech., 13, 3413–3445, https://doi.org/10.5194/amt-13-3413-2020, 2020.

Barbiero, R. P., James, W. F., and Barko, J. W.: The effects of disturbance events on phytoplankton community structure in a small temperate reservoir: Effects of disturbance on phytoplankton, Freshw. Biol., 42, 503–512, https://doi.org/10.1046/j.1365-2427.1999.00491.x, 1999.

Bertrand, G., Celle-Jeanton, H., Laj, P., Rangognio, J., and Chazot, G.: Rainfall chemistry: long range transport versus below cloud scavenging. A two-year study at an inland station (Opme, France), J. Atmospheric Chem., 60, 253–271, https://doi.org/10.1007/s10874-009-9120-y, 2008.

Burrows, S. M., Elbert, W., Lawrence, M. G., and Pöschl, U.: Bacteria in the global atmosphere – Part 1: Review and synthesis of literature data for different ecosystems, Atmospheric Chem. Phys., 9, 9263–9280, https://doi.org/10.5194/acp-9-9263-2009, 2009.

Callieri, C.: Single cells and microcolonies of freshwater picocyanobacteria: a common ecology, J. Limnol., 69, 257–277, https://doi.org/10.4081/jlimnol.2010.257, 2010.

Coumou, D. and Rahmstorf, S.: A decade of weather extremes, Nat. Clim. Change, 2, 491–496, https://doi.org/10.1038/nclimate1452, 2012.

Curren, E. and Leong, S. C. Y.: Natural and anthropogenic dispersal of cyanobacteria: a review, Hydrobiologia, 847, 2801–2822, https://doi.org/10.1007/s10750-020-04286-y, 2020.

Deguillaume, L., Charbouillot, T., Joly, M., Vaïtilingom, M., Parazols, M., Marinoni, A., Amato, P., Delort, A.-M., Vinatier, V., Flossmann, A., Chaumerliac, N., Pichon, J. M., Houdier, S., Laj, P., Sellegri, K., Colomb, A., Brigante, M., and Mailhot, G.: Classification of clouds sampled at the puy de Dôme (France) based on 10 yr of monitoring of their physicochemical properties, Atmospheric Chem. Phys., 14, 1485–1506, https://doi.org/10.5194/acp-14-1485-2014, 2014.

Dillon, K. P., Correa, F., Judon, C., Sancelme, M., Fennell, D. E., Delort, A.-M., and Amato, P.: Cyanobacteria and Algae in Clouds and Rain in the Area of puy de Dôme, Central France, Appl. Environ. Microbiol., https://doi.org/10.1128/AEM.01850-20, 2020.

Elliott, J. A.: The seasonal sensitivity of Cyanobacteria and other phytoplankton to changes in flushing rate and water temperature, Glob. Change Biol., 16, 864–876, https://doi.org/10.1111/j.1365-2486.2009.01998.x, 2010.

de Eyto, E., Jennings, E., Ryder, E., Sparber, K., Dillane, M., Dalton, C., and Poole, R.: Response of a humic lake ecosystem to an extreme precipitation event: physical, chemical, and biological implications, Inland Waters, 6, 483–498, https://doi.org/10.1080/IW-6.4.875, 2016.

Gaedeke, A. and Sommer, U.: The influence of the frequency of periodic disturbances on the maintenance of phytoplankton diversity, Oecologia, 71, 25–28, https://doi.org/10.1007/BF00377315, 1986.

Hughes, D. D., Mampage, C. B. A., Jones, L. M., Liu, Z., and Stone, E. A.: Characterization of Atmospheric Pollen Fragments during Springtime Thunderstorms, Environ. Sci. Technol. Lett., 7, 409–414, https://doi.org/10.1021/acs.estlett.0c00213, 2020.

Itahashi, S., Yumimoto, K., Uno, I., Hayami, H., Fujita, S., Pan, Y., and Wang, Y.: A 15-year record (2001–2015) of the ratio of nitrate to non-sea-salt sulfate in precipitation over East Asia, Atmospheric Chem. Phys., 18, 2835–2852, https://doi.org/10.5194/acp-18-2835-2018, 2018.

Jennings, E., Jones, S., Arvola, L., Staehr, P. A., Gaiser, E., Jones, I. D., Weathers, K. C., Weyhenmeyer, G. A., Chiu, C.-Y., and de Eyto, E.: Effects of weather-related episodic events in lakes: an analysis based on high-frequency data, 2012.

https://doi.org/10.5194/bg-2022-100
Preprint. Discussion started: 24 May 2022

Jöhnk, K. D., Huisman, J., Sharples, J., Sommeijer, B., Visser, P. M., and Stroom, J. M.: Summer heatwaves promote blooms of harmful cyanobacteria: HEATWAVES PROMOTE HARMFUL CYANOBACTERIA, Glob. Change Biol., 14, 495–512, https://doi.org/10.1111/j.1365-2486.2007.01510.x, 2008.

K. Sharma, N., K. Rai, A., and Singh, S.: Meteorological factors affecting the diversity of airborne algae in an urban atmosphere, Ecography, 29, 766–772, https://doi.org/10.1111/j.2006.0906-7590.04554.x, 2006.

Knapp, A. S. and Milewski, A. M.: Spatiotemporal Relationships of Phytoplankton Blooms, Drought, and Rainstorms in Freshwater Reservoirs, Water, 12, 404, https://doi.org/10.3390/w12020404, 2020.

Lange, P. A., Van der Graaf, G., and Gade, M.: Rain-induced subsurface turbulence measured using image processing methods, 3175 pp., https://doi.org/10.1109/IGARSS.2000.860374, 2000.

Lavrieux, M., Disnar, J.-R., Chapron, E., Bréheret, J.-G., Jacob, J., Miras, Y., Reyss, J.-L., Andrieu-Ponel, V., and Arnaud, F.: 6700 yr sedimentary record of climatic and anthropogenic signals in Lake Aydat (French Massif Central), The Holocene, 23, 1317–1328, https://doi.org/10.1177/0959683613484616, 2013.

Li, H. and Moisseev, D.: Two Layers of Melting Ice Particles Within a Single Radar Bright Band: Interpretation and Implications, Geophys. Res. Lett., 47, e2020GL087499, https://doi.org/10.1029/2020GL087499, 2020.

Luu, L. N., Vautard, R., Yiou, P., and Soubeyroux, J.-M.: Evaluation of convection-permitting extreme precipitation simulations for the south of France, Earth Syst. Dyn. Discuss., 1–24, https://doi.org/10.5194/esd-2020-77, 2020.

Negron, A., DeLeon-Rodriguez, N., Waters, S. M., Ziemba, L. D., Anderson, B., Bergin, M., Konstantinidis, K. T., and Nenes, A.: Using flow cytometry and light-induced fluorescence to characterize the variability and characteristics of bioaerosols in springtime in Metro Atlanta, Georgia, Atmospheric Chem. Phys., 20, 1817–1838, https://doi.org/10.5194/acp-20-1817-2020, 2020.

Padisák, J., Crossetti, L. O., and Naselli-Flores, L.: Use and misuse in the application of the phytoplankton functional classification: a critical review with updates, Hydrobiologia, 621, 1–19, https://doi.org/10.1007/s10750-008-9645-0, 2009.

Paerl, H. W. and Barnard, M. A.: Mitigating the global expansion of harmful cyanobacterial blooms: Moving targets in a human- and climatically-altered world, Harmful Algae, 96, 101845, https://doi.org/10.1016/j.hal.2020.101845, 2020.

Reichwaldt, E. S. and Ghadouani, A.: Effects of rainfall patterns on toxic cyanobacterial blooms in a changing climate: Between simplistic scenarios and complex dynamics, Water Res., 46, 1372–1393, https://doi.org/10.1016/j.watres.2011.11.052, 2012.

Renard, P., Bianco, A., Baray, J.-L., Bridoux, M., Delort, A.-M., and Deguillaume, L.: Classification of Clouds Sampled at the Puy de Dôme Station (France) Based on Chemical Measurements and Air Mass History Matrices, Atmosphere, 11, 732, https://doi.org/10.3390/atmos11070732, 2020.

Reynolds, C. S.: Phytoplankton assemblages and their periodicity in stratifying lake systems, Ecography, 3, 141–159, https://doi.org/10.1111/j.1600-0587.1980.tb00721.x, 1980.

Reynolds, C. S.: The Ecology of Phytoplankton, Cambridge University Press, 437 pp., 2006.

Reynolds, C. S., Huszar, V., Kruk, C., Naselli-Flores, L., and Melo, S.: Towards a functional classification of the freshwater phytoplankton, J. Plankton Res., 24, 417–428, https://doi.org/10.1093/plankt/24.5.417, 2002.

Richardson, J., Feuchtmayr, H., Miller, C., Hunter, P. D., Maberly, S. C., and Carvalho, L.: Response of cyanobacteria and phytoplankton abundance to warming, extreme rainfall events and nutrient enrichment, Glob. Change Biol., 25, 3365–3380, https://doi.org/10.1111/gcb.14701, 2019.

https://doi.org/10.5194/bg-2022-100
Preprint. Discussion started: 24 May 2022

Rinke, K., Yeates, P., and Rothhaupt, K.-O.: A simulation study of the feedback of phytoplankton on thermal structure via light extinction, Freshw. Biol., 55, 1674–1693, https://doi.org/10.1111/j.1365-2427.2010.02401.x, 2010.

Rooney, G. G., van Lipzig, N., and Thiery, W.: Estimating the effect of rainfall on the surface temperature of a tropical lake, Hydrol. Earth Syst. Sci., 22, 6357–6369, https://doi.org/10.5194/hess-22-6357-2018, 2018.

Rosas, I., Roy-Ocotla, G., and Mosiño, P.: Meteorological effects on variation of airborne algae in Mexico, Int. J. Biometeorol., 33, 173–179, https://doi.org/10.1007/BF01084602, 1989.

Šantl-Temkiv, T., Amato, P., Casamayor, E. O., Lee, P. K. H., and Pointing, S. B.: Microbial ecology of the atmosphere, FEMS Microbiol. Rev., fuac009, https://doi.org/10.1093/femsre/fuac009, 2022.

Schlichting, H. E.: Meteorological conditions affecting the dispersal of airborne algae and Protozoa, Am. J. Bot. 516 Pt, 2, 684, 1964.

Schmid, M., Hunziker, S., and Wüest, A.: Lake surface temperatures in a changing climate: a global sensitivity analysis, Clim. Change, 124, 301–315, https://doi.org/10.1007/s10584-014-1087-2, 2014.

Stocker, T. F. and Intergovernmental Panel on Climate Change (Eds.): Climate change 2013: the physical science basis ; summary for policymakers, a report of Working Group I of the IPCC, technical summary, a report accepted by Working Group I of the IPCC but not approved in detail and frequently asked questions ; part of the Working Group I contribution to the fifth assessment report of the Intergovernmental Panel on Climate Change, Intergovernmental Panel on Climate Change, New York, 203 pp., 2013.

Stockwell, J. D., Doubek, J. P., Adrian, R., Anneville, O., Carey, C. C., Carvalho, L., De Senerpont Domis, L. N., Dur, G., Frassl, M. A., Grossart, H., Ibelings, B. W., Lajeunesse, M. J., Lewandowska, A. M., Llames, M. E., Matsuzaki, S. S., Nodine, E. R., Nõges, P., Patil, V. P., Pomati, F., Rinke, K., Rudstam, L. G., Rusak, J. A., Salmaso, N., Seltmann, C. T., Straile, D., Thackeray, S. J., Thiery, W., Urrutia-Cordero, P., Venail, P., Verburg, P., Woolway, R. I., Zohary, T., Andersen, M. R., Bhattacharya, R., Hejzlar, J., Janatian, N., Kpodonu, A. T. N. K., Williamson, T. J., and Wilson, H. L.: Storm impacts on phytoplankton community dynamics in lakes, Glob. Change Biol., 26, 2756–2784, https://doi.org/10.1111/gcb.15033, 2020.

Tormo, R., Recio, D., Silva, I., and Muñoz, A. F.: A quantitative investigation of airborne algae and lichen soredia obtained from pollen traps in south-west Spain, Eur. J. Phycol., 36, 385–390, https://doi.org/10.1017/S0967026201003353, 2001.

Verspagen, J. M. H., Passarge, J., Jöhnk, K. D., Visser, P. M., Peperzak, L., Boers, P., Laanbroek, H. J., and Huisman, J.: Water management strategies against toxic Microcystis blooms in the Dutch delta, Ecol. Appl. Publ. Ecol. Soc. Am., 16, 313–327, https://doi.org/10.1890/04-1953, 2006.

Whitehead, P. G., Wilby, R. L., Battarbee, R. W., Kernan, M., and Wade, A. J.: A review of the potential impacts of climate change on surface water quality, Hydrol. Sci. J., 54, 101–123, https://doi.org/10.1623/hysj.54.1.101, 2009.

Wilhelm, S. and Adrian, R.: Impact of summer warming on the thermal characteristics of a polymictic lake and consequences for oxygen, nutrients and phytoplankton, Freshw. Biol., 53, 226–237, https://doi.org/10.1111/j.1365-2427.2007.01887.x, 2008.

Wiśniewska, K., Lewandowska, A. U., and Śliwińska-Wilczewska, S.: The importance of cyanobacteria and microalgae present in aerosols to human health and the environment – Review study, Environ. Int., 131, 104964, https://doi.org/10.1016/j.envint.2019.104964, 2019.

Wiśniewska, K. A., Śliwińska-Wilczewska, S., and Lewandowska, A. U.: Airborne microalgal and cyanobacterial diversity and composition during rain events in the southern Baltic Sea region, Sci. Rep., 12, 2029, https://doi.org/10.1038/s41598-022-06107-9, 2022.

Wood, S. A., Borges, H., Puddick, J., Biessy, L., Atalah, J., Hawes, I., Dietrich, D. R., and Hamilton, D. P.: Contrasting cyanobacterial communities and microcystin concentrations in summers with extreme weather events:

https://doi.org/10.5194/bg-2022-100
Preprint. Discussion started: 24 May 2022

780 insights into potential effects of climate change, Hydrobiologia, 785, 71–89, https://doi.org/10.1007/s10750-016-2904-6, 2017.

Woolway, R. I. and Merchant, C. J.: Worldwide alteration of lake mixing regimes in response to climate change, Nat. Geosci., 12, 271–276, https://doi.org/10.1038/s41561-019-0322-x, 2019.

Yang, Z., Zhang, M., Shi, X., Kong, F., Ma, R., and Yu, Y.: Nutrient reduction magnifies the impact of extreme
785 weather on cyanobacterial bloom formation in large shallow Lake Taihu (China), Water Res., 103, 302–310, https://doi.org/10.1016/j.watres.2016.07.047, 2016.

Zhu, M., Paerl, H. W., Zhu, G., Wu, T., Li, W., Shi, K., Zhao, L., Zhang, Y., Qin, B., and Caruso, A. M.: The role of tropical cyclones in stimulating cyanobacterial (Microcystis spp.) blooms in hypertrophic Lake Taihu, China, Harmful Algae, 39, 310–321, https://doi.org/10.1016/j.hal.2014.09.003, 2014.

790 Znachor, P., Zapomělová, E., Řeháková, K., Nedoma, J., and Šimek, K.: The effect of extreme rainfall on summer succession and vertical distribution of phytoplankton in a lacustrine part of a eutrophic reservoir, Aquat. Sci., 70, 77–86, https://doi.org/10.1007/s00027-007-7033-x, 2008.